

43. Fluctuating Double-Bond Localization and Charge Migration in π Systems

by Edgar Heilbronner^{a)}* and Sason Shaik^{b)}

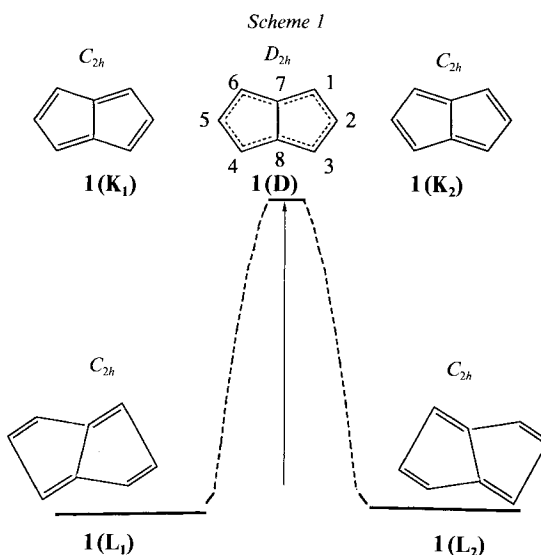
^{a)} Grütstrasse 10, CH-8704 Herrliberg

^{b)} Department of Chemistry, Ben Gurion University of the Negev, P.O.B. 653, 84105 Beer Sheva, Israel

(28.1.92)

In π systems with localized double bonds, the switch from one localization pattern to another symmetry-equivalent one, and the corresponding changes in electron distribution are often considered to proceed *via* a delocalized transition state of higher symmetry. We present a different mechanism, according to which the double-bond localization and the concomitant charge distributions can fluctuate without change in energy and *without* passing through a delocalized, higher-symmetry transition state. This result is obtained within a simple, independent-electron (HMO-type) treatment.

1. Introduction. – Many molecules, in particular those with non-alternant π systems, for which a series of *Kekulé* formulae (**K**) can be written, prefer to localize their double bonds, and distort according to a structure (**L**) close to one of these *Kekulé* formulae, instead of assuming a delocalized structure (**D**) corresponding to their (weighted) superposition [1]. A classical example is pentalene **1** [2] (*cf.* Scheme 1), where the C_{2h} -localized structures **1(L₁)** and **1(L₂)** lie energetically lower than the D_{2h} structure **1(D)**, which may be roughly described as the resonance hybrid **1(K₁)** \leftrightarrow **1(K₂)**. The latter is the transition state



for the valence tautomerism or the bond-switching reactions $\mathbf{1}(\mathbf{L}_1) \rightarrow \mathbf{1}(\mathbf{D}) \rightarrow \mathbf{1}(\mathbf{L}_2)$ and $\mathbf{1}(\mathbf{L}_2) \rightarrow \mathbf{1}(\mathbf{D}) \rightarrow \mathbf{1}(\mathbf{L}_1)$, which need a substantial activation energy E^\ddagger of $\sim 15 \text{ kJ} \cdot \text{mol}^{-1}$, as indicated qualitatively in *Scheme 1* [3].

Usually, but not always¹⁾ (*cf.* [2]), such a double-bond localization (DBL) is accompanied by a reduction of symmetry, relative to the energetically less favorable delocalized structure, *e.g.* in the case of the structures $\mathbf{1}(\mathbf{L}_1)$ and $\mathbf{1}(\mathbf{L}_2)$ relative to $\mathbf{1}(\mathbf{D})$.

The double-bond localization (DBL) is equivalent to a redistribution of charge, *e.g.* in the case of $\mathbf{1}(\mathbf{D}) \rightarrow \mathbf{1}(\mathbf{L}_1)$ or $\mathbf{1}(\mathbf{L}_2)$ an increase in charge density at C(1), C(3), C(4), and C(6), a decrease at centres at C(2), C(5), C(7), and C(8), and an increase (decrease) in overlap population for the double (single) π bonds in $\mathbf{1}(\mathbf{L}_1)$ and $\mathbf{1}(\mathbf{L}_2)$ relative to the charge distribution in $\mathbf{1}(\mathbf{D})$. The mechanism of such charge shifts (electron transfer, bond shifts, conductivity in large systems) is a fundamental problem in contemporary chemistry, and has received much attention in studies of electron transfer and of conductivity in crystals and polymers [4–6].

To gain an insight into the rules which govern such charge shifts, one must first understand the mechanism leading to, or preventing DBL in a molecule.

Consider the benzene molecule. Here, the delocalized D_{6h} structure is an absolute minimum on the energy hypersurface. The π -localized D_{3h} structures lie higher in energy, and none of them (with exception of the limiting case of three acetylenes) corresponds even to a local minimum.

It follows that, if we are looking for molecules possessing a low-energy pathway for charge migration, we must look for molecules undergoing spontaneous DBL, but which nevertheless offer a low-activation-energy path for switching from one localized structure to another.

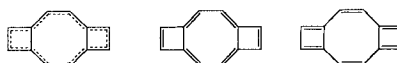
In this paper, we propose a mechanism for charge redistribution, which allows the passage from one localized structure \mathbf{L}_1 to other localized structures \mathbf{L}_i without passing through a delocalized structure \mathbf{D} of higher energy, *i.e.*, without (significant) activation energy. Our model is based on second-order perturbation theory within the *Hückel* formalism [7] (*see Appendix*).

2. Double-Bond Localization and Charge Shifts in π Systems. – The model treatment, its advantages, and its inherent disadvantages have been already described in detail [7]. (It is briefly presented in the *Appendix*, where the relevant formulae have been numbered *A1*, *A2*, *etc.*) A short summary of the assumptions involved may be helpful.

The results to be discussed below are obtained by a four-step procedure as follows:

1) A standard HMO calculation is performed for the π system of the molecule, assuming maximal symmetry of the graph \mathfrak{G} representing its topography, and assuming all bond-lengths equal, *i.e.* $R_{\mu\nu} = R_0$. Although the exact value of R_0 is irrelevant at this stage, we assume that it corresponds to that of a benzene π bond of bond-order $p_0 = 2/3$, *i.e.* $R_0 \approx 140 \text{ pm}$ (*cf.* *A6*), to which we assign a standard resonance integral β_0 . This calculation yields the HMOs φ_i (*A1*), the corresponding orbital energies ε_i (*A2*), the bond-orders $p_{\mu\nu}$ (*A4*), and the bond-bond polarizabilities $\pi_{\mu\nu,\rho\sigma}$ (*A9*), the latter collected in the matrix $\boldsymbol{\pi} = (\pi_{\mu\nu,\rho\sigma})$.

¹⁾ Thus, the hypothetical, planar dicyclobuta[*a,e*]-cyclooctene (**2**) has D_{2h} symmetry, both in its delocalized **2(D)** and in its localized structures **2(L)**:



II) First-Order DBL. We define as first-order DBL, the change $\delta R_{\mu\nu}$ of each of the individual bond-lengths $R_{\mu\nu}$ from the assumed standard length R_0 to a length $R_{\mu\nu}^0$ defined by the individual bond-orders $p_{\mu\nu}$ according to $R_{\mu\nu}^0 = R_0 + r(p_{\mu\nu} - 2/3)$ (cf. A5, A6). This assumes that each bond-length change $\delta R_{\mu\nu}$ can be adjusted *independently* of the changes $\delta R_{\rho\sigma}$ in the other bond-lengths $R_{\rho\sigma}$. An important consequence is that *first-order DBL conserves the original symmetry of the structure underlying step I.*

III) Second-Order DBL. Second-order DBL, *i.e.* the changes of the bond-lengths $R_{\mu\nu}$ relative to the values $R_{\mu\nu}^0$ computed in step *II*, is obtained according to the procedure outlined in the *Appendix*, *i.e.* by diagonalizing the bond-bond polarizability matrix $\boldsymbol{\pi}$ (A11). This yields two results:

a) The largest eigenvalue λ_{\max} (A12) of $\boldsymbol{\pi}$ determines, if the molecule will undergo second-order DBL, depending on whether $\lambda_{\max} > \lambda_{\text{critical}}$, or $\lambda_{\max} < \lambda_{\text{critical}}$ (A14), where $\lambda_{\text{critical}}$ is a critical value, estimated [7] to be in the range $1.7 < \lambda_{\text{critical}} < 1.8$.

b) The components $u_{\max,\mu\nu}$ of the eigenvector \mathfrak{w}_{\max} of $\boldsymbol{\pi}$ corresponding to λ_{\max} (cf. A13) yield estimates of the second-order DBL bond-length changes relative to $R_{\mu\nu}^0$. These changes $\delta R_{\mu\nu} = R_{\mu\nu} - R_{\mu\nu}^0$ are proportional to the changes $\delta p_{\mu\nu} = f_{\text{eq}} \cdot u_{\max,\mu\nu}$ in the bond-orders, where f_{eq} is a factor of unspecified sign. Note that the individual changes $\delta R_{\mu\nu}$ now include the dependence on the changes $\delta R_{\rho\sigma}$ in *all* the other bonds $\rho\sigma \neq \mu\nu$.

IV) The size of f_{eq} yielding estimates of $R_{\mu\nu,\text{eq}}$, *i.e.* of the equilibrium structure of the molecule, depends on higher-order terms not considered in our treatment. Assuming an *ad hoc* estimate for f_{eq} and thus for δ_{eq} (cf. formulae A15–A17 of the *Appendix*), yields the desired equilibrium-structure bond-orders $p_{\mu\nu,\text{eq}}$, which in turn determine the equilibrium interatomic distances $R_{\mu\nu,\text{eq}}$, and thus the appropriate values of the resonance integrals

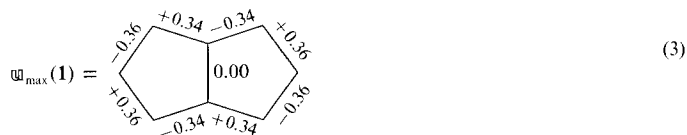
$$\beta_{\mu\nu,\text{eq}} = \beta_0(1 + \delta_{\mu\nu,\text{eq}}), \quad (1)$$

where the correction terms are given in a sufficient approximation by

$$\delta_{\mu\nu,\text{eq}} = (2/3)(p_{\mu\nu} - 2/3) + u_{\max,\mu\nu}/2 \quad (2)$$

as shown in the *Appendix* (A17). With these new values of $\beta_{\mu\nu,\text{eq}}$, one runs a further HMO calculation, which yields the corresponding charge orders $q_{\mu,\text{eq}}$ and thus – by comparison with the original q_{μ} values – the charge drifts $q_{\mu,\text{eq}} - q_{\mu}$ due to second-order DBL. (The peculiarities of the HMO formalism, concerning charge distributions in π systems are discussed in the *Appendix*, cf. formulae A18–A20.)

For pentalene (**1**), the standard HMO calculation (all $\beta_{\mu\nu} = \beta_0$) yields the bond orders $p_{1,2} = 0.650$, $p_{1,7} = 0.524$, and $p_{7,8} = 0.531$, which determine the first-order DBL, as well as the charge orders $q_1 = 0.815$, $q_2 = 1.173$, and $q_7 = 1.198$. The largest eigenvalue of the bond-bond polarizability matrix $\boldsymbol{\pi}(\mathbf{1})$ is $\lambda_{\max} = 2.357$, which is larger than $\lambda_{\text{critical}} \approx 1.8$. From this, we conclude that **1** undergoes second-order DBL. The corresponding eigenvector $\mathfrak{w}_{\max}(\mathbf{1})$ is shown here graphically, where the numbers correspond to the individual components $u_{\max,\mu\nu}$:



This means that second-order DBL leads to a stabilization of **1** by a bond-alternation mode, reducing the symmetry of the molecule from D_{2h} to C_{2h} .

We now compute the correction terms $\delta_{\mu\nu,\text{eq}}$, using Eqn. 2, which yield, according to Eqn. 1 the following resonance-integral ratios:

μ, ν	1.2	1.7	2.3	3.8	7.8	(4)
$\beta_{\mu\nu,\text{eq}}/\beta_0$	1.17	0.73	0.81	1.07	0.90	

A HMO calculation with these parameters gives the following charge orders $q_{\mu,\text{eq}}$ which, compared with the original values q_μ , yield the charge-order shifts $\Delta q_\mu = q_{\mu,\text{eq}} - q_\mu$ that accompany the second-order DBL:

μ	1	2	3	7	(5)
$q_{\mu,\text{eq}}$	0.970	1.064	0.867	1.098	
q_μ	0.815	1.173	0.815	1.198	
Δq_μ	+0.155	-0.109	+0.052	-0.100	

The charge shifts correspond to a trend towards local neutrality, *i.e.* the $q_{\mu,\text{eq}}$ for $\mathbf{1}(\mathbf{L}_1)$ or $\mathbf{1}(\mathbf{L}_2)$ are closer to unity than the q_μ of the delocalized structure $\mathbf{1}(\mathbf{D})$. The bond-orders ($p_{1,2} = 0.891, p_{3,8} = 0.802, p_{1,7} = 0.272, p_{2,3} = 0.361, p_{7,8} = 0.427$) show that this particular DBL pattern corresponds to $\mathbf{1}(\mathbf{L}_2)$ given in Scheme 1.

In principle, steps I–IV should be iterated, until self-consistency in charge- and bond-orders is reached. However, this is hardly warranted in view of the crudeness of the model. Furthermore, it has been shown [8] that inclusion of electron-electron interaction into the above scheme does not yield results which are significantly different. On the whole, the same seems to be true for many-electron treatments of DBL, initiated mainly by Dewar *et al.* [9].

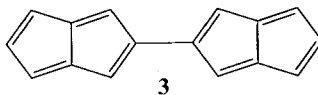
Although the above formalism involves all the HMO π orbitals, the type of distortion can often be obtained from the direct product $\Gamma(\text{HOMO}) \otimes \Gamma(\text{LUMO})$ of the irreducible representations to which the HOMO and LUMO belong [10]. This is similar to a treatment of the pseudo-Jahn-Teller effect [11], which considers the stabilization of the molecule arising from a distortion along the normal mode which most efficiently couples the ground state with excited states of another symmetry. The excited state, which offers the most efficient stabilization, corresponds, on a molecular-orbital level, to the one dominated by the HOMO \rightarrow LUMO configuration, and the corresponding distortion mode is again determined by the direct product $\Gamma(\text{HOMO}) \otimes \Gamma(\text{LUMO})$. A similar treatment has been proposed by Nakajima *et al.* [12]. For pentalene ($\mathbf{1}$), the HOMO and LUMO belong to the irreducible representations B_{1u} and A_u , respectively, and the direct product $B_{1u} \otimes A_u = B_{1g}$ indeed describes the distortion mode, shown in (3). The reason, why the HOMO and LUMO play a decisive role here, is the small orbital-energy gap $\epsilon_{\text{LUMO}} - \epsilon_{\text{HOMO}}$ between the two orbitals. This is often the case in molecules undergoing second-order DBL (see A9 in Appendix).

3. Fluctuating Double-Bond Localization²⁾. – In the mechanism we now present, the localized structures \mathbf{L}_i , (*e.g.* \mathbf{L}_1 and \mathbf{L}_2) are more stable than the delocalized structure \mathbf{D} (*i.e.*

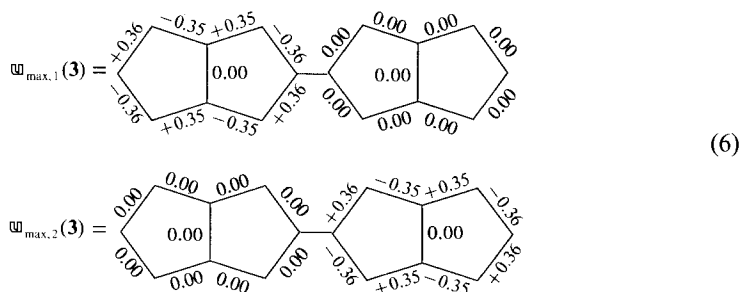
²⁾ Before we discuss examples of fluctuating DBL, we should state briefly what we do not wish to include under this heading. Quite apart from molecules with a fluctuating structure, where localized double and single bonds are cleaved and formed in a concerted reaction, *e.g.* in bullvalene, we also exclude the limiting case $\lambda_{\text{max}} = \lambda_{\text{critical}}$ (*cf.* criterion A14 in Appendix). Under this condition, the delocalized structure \mathbf{D} and the localized structures \mathbf{L}_1 and \mathbf{L}_2 are accidentally degenerate, so that the transition from \mathbf{L}_1 to \mathbf{L}_2 proceeds – as far as our model is concerned (*cf.* [7]) – without activation energy, but still *via* the delocalized transition state \mathbf{D} of higher symmetry.

$\lambda_{\max} > \lambda_{\text{critical}}$), and at the same time can interconvert into each other without passing through a higher-energy transition state in particular without passing through the delocalized structure **D**. This mechanism is explained with reference to two particular examples.

3.1. *Neutral Systems. Example: 2,2'-Bipentalenyl (3)*. Here, the bond-bond polarizability matrix $\pi(\mathbf{3})$, of order 19×19 , yields as largest eigenvalue $\lambda_{\max}(\mathbf{3}) = 3.026$. Thus, by



linking C(2) and C(2') of the two pentalene moieties, the tendency towards DBL has increased with respect to that of the parent pentalene **1** ($\lambda_{\max}(\mathbf{1}) = 2.357$). However, a more remarkable result is that *this eigenvalue is degenerate*, the two corresponding, normalized eigenvectors $\mathfrak{w}_{\max,1}(\mathbf{3})$ and $\mathfrak{w}_{\max,2}(\mathbf{3})$ having the following form:



The eigenvector $\mathfrak{w}_{\max,1}(\mathbf{3})$ corresponds to DBL in the left pentalene moiety, and the eigenvector $\mathfrak{w}_{\max,2}(\mathbf{3})$ to DBL in the right one. In each case, the other moiety *remains delocalized*, as described by first-order DBL. Since the two particular solutions shown in (6) are degenerate, any linear combination is also a solution with the same value $\lambda_{\max}(\mathbf{3})$. Thus, we can form the mutually orthogonal pair of general, normalized solutions (7), where the angle ω can take any value between $0 \leq \omega < 2\pi$:

$$\begin{aligned} \mathfrak{w}_{\max}(\mathbf{3}) &= \mathfrak{w}_{\max,1}(\mathbf{3}) \cos \omega + \mathfrak{w}_{\max,2}(\mathbf{3}) \sin \omega \\ \mathfrak{w}_{\max}(\mathbf{3})' &= \mathfrak{w}_{\max,1}(\mathbf{3}) \sin \omega - \mathfrak{w}_{\max,2}(\mathbf{3}) \cos \omega. \end{aligned} \quad (7)$$

All these solutions, including $\mathfrak{w}_{\max,1}(\mathbf{3})$ ($\omega = 0$) and $\mathfrak{w}_{\max,2}(\mathbf{3})$ ($\omega = \pi/2$) shown in (6), correspond to DBL patterns $\mathbf{3}(\mathbf{L}_\omega)$ well away from the fully delocalized structure $\mathbf{3}(\mathbf{D})$ of **3**. In fact, the linear combinations (7) imply that we can pass from a particular localization pattern $\mathbf{3}(\mathbf{L}_\omega)$, determined by some value of the angle ω , to any other pattern $\mathbf{3}(\mathbf{L}_{\omega'})$ corresponding to a different angle $\omega' \neq \omega$, *without change in energy*. In the Figure is shown how the localization pattern $\mathbf{3}(\mathbf{L}_\omega)$ depends on ω . Strong DBL switches from one side of the molecule to the other, passing through patterns where both sides exhibit weakened DBL. In these intermediate situations, both components $\mathfrak{w}_{\max,1}(\mathbf{3})$ and $\mathfrak{w}_{\max,2}(\mathbf{3})$ in (7) are weighted by $|\cos \omega| < 1$ or $|\sin \omega| < 1$, e.g. by $1/\sqrt{2}$ if $\omega = \pi/4$. In this whole process, the itinerary never passes through the high-energy, fully delocalized structure $\mathbf{3}(\mathbf{D})$, the centre of the circle shown in the Figure.

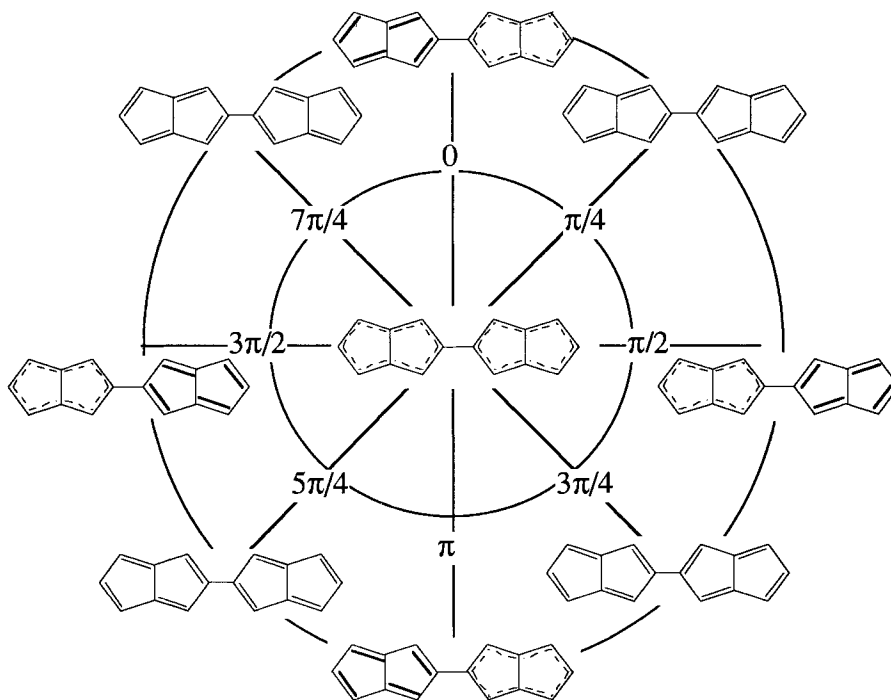
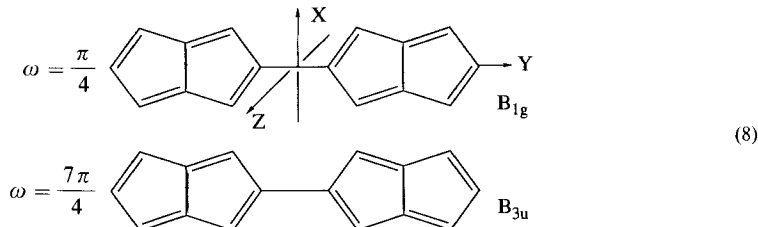


Figure. Degenerate DBL fluctuation in 2,2'-bipentalenyl (**3**) and its radical cation 3^+ . Dotted lines in a pentalene unit indicate that it is delocalized and has local D_{2h} symmetry with bond lengths corresponding to first-order DBL, i.e. according to the bond orders $p_{\mu\nu}$. Alternating double and single bonds indicate the presence of second-order DBL. Bold double bonds correspond to shorter, more strongly localized double bonds. In the case of the radical cation 3^+ , the positive charge is located preferentially on the delocalized pentalene unit. The indicated values of the angle ω refer to formula (7).

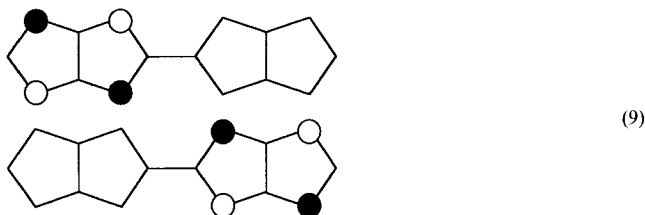
Whereas our simple HMO treatment predicts that the process depicted in the *Figure* proceeds without any activation energy, the presence of small barriers can obviously not be excluded. However, such barriers should be much smaller than the activation energy E^\ddagger for the bond-switching process in pentalene **1**. If they are within the range of zero-point energies of normal vibration modes corresponding to the distortions (6) or (7), then these vibrations will cause the DBL in **3** to oscillate from one pentalene unit to the other in a non-activated manner.

In the case of **3** (and for similar molecules), the symmetry argument presented in context of pentalene **1**, runs into a subtle difficulty. The graph \mathfrak{G} of molecule **3** is of symmetry D_{2h} , assuming the molecule to be planar. Whereas the canonical HOMO of **3** ($\epsilon_{\text{HOMO}} = \alpha$) is non-degenerate and belongs to the irreducible representation B_{3g} , there is a pair of degenerate, canonical LUMOs ($\epsilon_{\text{LUMO}} = \alpha + 0.206\beta$) belonging to B_{2g} and A_u , respectively. The small HOMO/LUMO gap might suggest that the DBL pattern is determined mainly by the symmetry behavior of these orbitals. Accordingly, the predicted DBL patterns should belong either to the irreducible representations $B_{2g} \otimes B_{3g} = B_{1g}$ or $A_u \otimes B_{3g} = B_{3u}$. This is indeed the case as shown in the following dia-

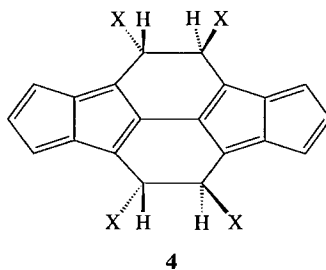
grams, which are identical to those in the *Figure* for $\omega = \pi/4$ and $\omega = 7\pi/4$. But it is not obvious from this argument that these patterns should correspond to the same eigenvalue $\lambda_{\max}(\mathbf{3}) = 3.026$ of the bond-bond polarizability matrix $\mathbf{\pi}(\mathbf{3})$. Note that the in-phase and out-of-phase linear combinations of the patterns (8) do indeed correspond to the eigenvectors $\mathbf{w}_{\max,1}(\mathbf{3})$ and $\mathbf{w}_{\max,2}(\mathbf{3})$ shown in (6).



An alternative procedure would have been to assign to the two accidentally degenerate LUMOs of **3** the semi-localized orbitals (9) having finite coefficients in only one or the other of the two pentalene moieties. These orbitals, which do not reflect the D_{2h} symmetry of the molecule, suggest, however, that the DBL pattern should conform to the eigenvectors of (6).



An amusing consequence of the situation depicted in the *Figure* is that an appropriately substituted 2,2'-bipentalenyl (**4**), in which the substituents X are assumed to be locally achiral (*e.g.* Cl-atoms), would be chiral for all values of ω describing its DBL, with the exception of $\omega = \pi/4$ and $\omega = 5\pi/4$, for which it has C_i symmetry, *i.e.* as depicted below. Thus, **4** would switch, without changing its energy, from one enantiomer to its mirror image. This is a special case of a narcissistic reaction [13], not needing any activation energy.



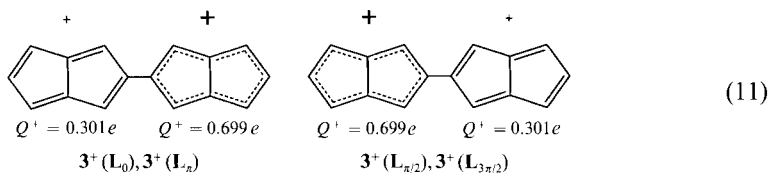
3.2. Charged Systems. Example: 2,2'-Bipentalenyl Radical Cation. Removal of an electron from the HOMO of pentalene **1** yields its radical cation $\mathbf{1}^+$ in the electronic ground state. The largest eigenvalue of the bond-bond polarizability matrix $\mathbf{\pi}(\mathbf{1}^+)$ is now $\lambda_{\max} = 1.358$, which is smaller than $\lambda_{\text{critical}}$ (condition A14 in *Appendix*). Consequently, $\mathbf{1}^+$ does not undergo DBL, but preserves its maximal D_{2h} symmetry.

On the other hand, the matrix $\boldsymbol{\pi}(\mathbf{3}^+)$ of the 2,2'-bipentalenyl radical cation $\mathbf{3}^+$ in its electronic ground state yields $\lambda_{\max}(\mathbf{3}^+) = 2.040$ which does satisfy condition *A14* (see *Appendix*), implying that the fully delocalized radical cation $\mathbf{3}^+(\mathbf{D})$ lies above the delocalized one in energy. Again, $\lambda_{\max}(\mathbf{3}^+) = 2.040$ is a degenerate eigenvalue, the components of its eigenvectors $\boldsymbol{\Psi}_{\max,1}(\mathbf{3}^+)$ and $\boldsymbol{\Psi}_{\max,2}(\mathbf{3}^+)$ being practically those of $\boldsymbol{\Psi}_{\max,1}(\mathbf{3})$ and $\boldsymbol{\Psi}_{\max,2}(\mathbf{3})$ shown in (6). It follows that our conclusions about DBL in $\mathbf{3}$ are equally valid for $\mathbf{3}^+$. In particular, the linear combinations (7) again yield the cycle of localization patterns shown in the *Figure*.

The only novel feature concerns the changes in charge distribution which accompany the fluctuation of DBL. In the absence of DBL, the positive unit charge e is distributed over the delocalized radical cation $\mathbf{3}(\mathbf{D})$ according to (*cf. A18–A19, Appendix*)

$$Q_{\mu}^+ = e - Q_{\mu} = e(1 - q_{\mu}) \quad (10)$$

with $\sum_{\mu} Q_{\mu}^+ = e$. This frozen charge distribution is totally symmetric with respect to the symmetry operations of D_{2h} . When second-order DBL sets in, the charge distribution depends on ω , and thus fluctuates with the localization patterns. A procedure for calculating the charge distribution Q_{μ} , and thus of Q_{μ}^+ , for a given set of values $u_{\max,\mu\nu}(\omega)$ obtained from (7), is described in *Appendix (A15–A17)*. Results for the special values $\omega = 0, \pi/2, \pi, 3\pi/2$, *i.e.* when the second-order DBL nests completely in one or the other of the pentalene moieties, are shown in (11), where the net positive charges Q^+ have been obtained by summing over the centres μ in the pentalene units:



It is seen that the odd electron, and thus the positive charge, prefers to nest on the delocalized moiety of $\mathbf{3}^+$, as might have been expected from the result that $\mathbf{1}^+$ itself prefers to be delocalized. If the charge localization proceeds as in (11), then an excess positive charge of $0.40e$ will oscillate between the two molecular halves in phase with the fluctuation of second-order DBL. Again, this movement proceeds along a quasi-equienergetic path. According to our model, this type of ‘charge transfer’ or partial ‘electron transfer’ is not an abrupt event, but a continuous wave-like process arising from the degeneracy of all possible DBL patterns $\mathbf{3}^+(\mathbf{L}_{\omega})$ described by (7)³.

Of course, the changes of localization pattern in the neutral parent $\mathbf{3}$ are also accompanied by changes in the Q_{μ} values, which now satisfy $\sum_{\mu} Q_{\mu} = 0$. For $\omega = 0$ (*cf. Fig.*), the net charge on the localized (left) pentalene unit is $Q_{\text{loc}} = 0.048e$ and on the (right) delocalized one $Q_{\text{deloc.}} = 0.048e$. As expected, the size of charge separation in the neutral molecule $\mathbf{3}$ is significantly smaller than the charge transfer in radical cation $\mathbf{3}^+$.

³) This process differs from the ‘sudden polarization’ discovered and discussed by *Salem* and coworkers [14]. In terms of our model, ‘sudden polarization’ occurs as the result of an accidental HOMO/LUMO degeneracy forced by structural changes, such as those accompanying the formation of an activated reaction complex. Under the condition $\varepsilon_{\text{HOMO}} = \varepsilon_{\text{LUMO}}$, the bond-bond polarizabilities (A9) become infinite, the denominator $\varepsilon_{\text{LUMO}} - \varepsilon_{\text{HOMO}}$ being zero. Obviously, this implies that $\lambda_{\max} = \infty$.

4. Polypentalenyls and Their Radical Cations. – Using the same treatment, we now examine how the number of repeating moieties in a linear chain will affect second-order DBL. For consistency, we use again pentalene units as building blocks to form 2,2':5',2''-terpentalenyl $\mathbf{5}_3$, 2,2':5',2'':5'',2'''-quaterpentalenyl $\mathbf{4}_4$, and 2,2':5',2'':5'',2''':5''',2''''-quinquepentalenyl $\mathbf{5}_5$, and their radical cations $\mathbf{5}_N^+$ (cf. Scheme 2). Note that $\mathbf{5}_1 \equiv \mathbf{1}$ = pentalene, and $\mathbf{5}_2 \equiv \mathbf{3}$ = 2,2'-bipentalenyl. Table 1 lists those eigenvalues λ_i of the bond-bond polarizability matrices $\boldsymbol{\pi}(\mathbf{5}_N)$ and $\boldsymbol{\pi}(\mathbf{5}_N^+)$, $N = 1, 2, 3, 4,$ and 5 , which exceed $\lambda_{\text{critical}}$ (A14, Ap-

Scheme 2

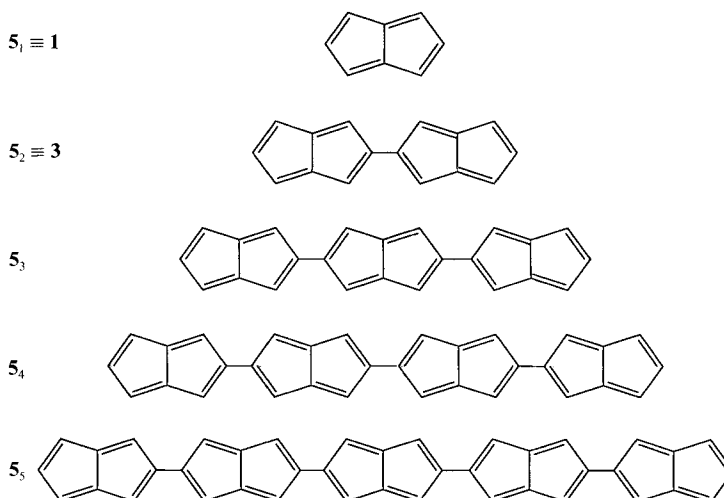


Table 1. Eigenvalues λ_i of the Bond-Bond Polarizability Matrices $\boldsymbol{\pi}(N)$ of the Polypentalenyls $\mathbf{5}_N$ and of Their Radical Cations $\mathbf{5}_N^+$ with $N = 1, 2, 3, 4,$ and 5 . Only the eigenvalues satisfying condition (A14) (Appendix) are given. The largest eigenvalue λ_{max} is given in italics. The corresponding eigenvectors \mathbf{u}_i are given symbolically as the DBL patterns, **L** and **D** designating a pentalene unit with or without DBL, respectively.

Molecule	λ_i	Radical cation	λ_i	DBL Pattern
$\mathbf{5}_1$	2.357	$\mathbf{5}_1^+$	1.358	L
$\mathbf{5}_2$	3.026	$\mathbf{5}_2^+$	2.040	L-D
	3.026		2.040	D-L
$\mathbf{5}_3$	4.361	$\mathbf{5}_3^+$	2.625	D-L-D
	3.359		2.528	L-D-D
	3.359		2.528	D-D-L
$\mathbf{5}_4$	5.161	$\mathbf{5}_4^+$	3.252	D-L-D-D
	5.161		3.252	D-D-L-D
	3.559		2.855	L-D-D-D
	3.559		2.855	D-D-D-L
$\mathbf{5}_5$	6.362	$\mathbf{5}_5^+$	3.856	D-D-L-D-D
	5.695		3.825	D-L-D-D-D
	5.695		3.825	D-D-D-L-D
	3.693		3.085	L-D-D-D-D
	3.693		3.085	D-D-D-D-L

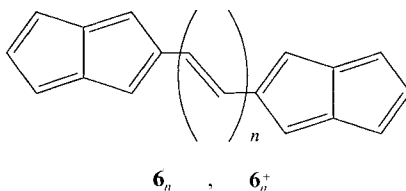
pendix). In addition, the corresponding eigenvectors \mathfrak{W}_i are symbolically represented by the corresponding DBL patterns, **L** and **D** standing for a pentalene moiety with or without double-bond alternation, respectively, as shown explicitly for $\mathbf{5}_2 \equiv \mathbf{3}$ in (6).

One notes that λ_{\max} is degenerate for even N , but single if N is odd. The number of λ_i values which satisfy criterion (A14), i.e. $\lambda_i > \lambda_{\text{critical}}$, equals the number N of pentalene units in the particular polypentalenyl chain. The remaining λ_i values (not listed) are smaller than 0.6, i.e. well below $\lambda_{\text{critical}} \approx 1.8$ to 1.9.

The corresponding eigenvectors $\mathfrak{W}_{\max}(\mathbf{5}_N)$ and $\mathfrak{W}_{\max}(\mathbf{5}_N^+)$ (Table 1) show that the second-order DBL involves only the central pentalene unit, if N is odd, or the innermost pair of rings, if N is even and λ_{\max} thus degenerate. It follows that, for even N , a general eigenvector can be written in analogy to (7), and that DBL will fluctuate in a similar fashion to that shown in the Figure for $\mathbf{5}_2 \equiv \mathbf{3}$. DBL in the remaining (outer) pentalene units will need some activation energy relative to the preferred DBL described by $\mathfrak{W}_{\max}(\mathbf{5}_N)$ or $\mathfrak{W}_{\max}(\mathbf{5}_N^+)$. This energy will depend on the size of the corresponding λ_i values, but will be much smaller than the energy needed to reach the situation in which all pentalene units are delocalized. Accordingly, it is still possible for DBL to fluctuate over all pentalene units without passing through a completely delocalized transition state. Whether the fluctuations described by eigenvectors $\mathfrak{W}_i(\mathbf{5}_N)$ – or $\mathfrak{W}_i(\mathbf{5}_N^+)$ – belonging to different eigenvalues λ_i are synchronized or not, will depend on the vibrational modes which link the fluctuation patterns. In a first approximation, the relative number of molecules exhibiting one or the other of the DBL patterns will be given by a Boltzmann distribution.

As discussed in connection with the radical cation $\mathbf{5}_2^+ \equiv \mathbf{3}^+$, the positive charge of the radical cations $\mathbf{5}_N^+$ tends to avoid the localized pentalene unit and to spread itself over the remaining ones. Thus, with increasing number N of linked pentalenes, the magnitude of the fluctuating charge will become smaller. Apart from that, all other remarks made in connection with $\mathbf{5}_2^+ \equiv \mathbf{3}^+$ remain valid.

5. 1, ω -Di(pentalen-2-yl)polyenes and Their Radical Cations. – To avoid the spreading of charge over N linked pentalene units, as described in the last paragraph for the radical cations $\mathbf{5}_N^+$, we examine briefly the case where only two pentalene moieties are linked at C(2) and (C2') via an alternant π system. The simplest examples of this type consist of polyene chains of n double bonds, carrying a pentalen-2-yl group at both ends, e.g. $\mathbf{6}_1 = 1,2$ -di(pentalen-2-yl)ethene, $\mathbf{6}_2 = 1,4$ -di(pentalen-2-yl)buta-1,3-diene, $\mathbf{6}_3 = 1,6$ -di(pentalen-2-yl)hexa-1,3,5-triene, $\mathbf{6}_4 = 1,8$ -di(pentalen-2-yl)octa-1,3,5,7-tetraene, and the corresponding radical cations $\mathbf{6}_n^+$ ($\mathbf{6}_0$ is identical to $\mathbf{3}$).



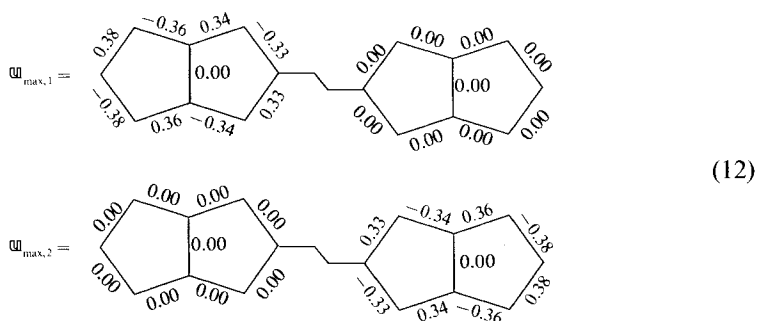
Diagonalization of the bond-bond polarizability matrices $\boldsymbol{\pi}(\mathbf{6}_n)$ and $\boldsymbol{\pi}(\mathbf{6}_n^+)$ for $n = 0$ to 4, yields the degenerate eigenvalues λ_{\max} listed in Table 2. Again, all λ_{\max} values are significantly larger than $\lambda_{\text{critical}}$, thereby satisfying the criterion (A14) (Appendix). Further-

Table 2. Eigenvalues λ_i of the Bond-Bond Polarizability Matrices $\mathbb{M}(n)$ of the 1, ω -Di(pentalen-2-yl)polyenes $\mathbf{6}_n$ and of their Radical Cations $\mathbf{6}_n^+$ with $n = 1, 2, 3$, and 4. The doubly degenerate eigenvalues λ_{\max} , satisfying condition (A14) (Appendix), are given in italics. All other eigenvalues, of which only $\lambda_{\max-1}$ is shown, are much smaller than $\lambda_{\text{critical}}$.

Molecule	λ_{\max}	$\lambda_{\max-1}$	Radical cation	λ_{\max}	$\lambda_{\max-1}$
$\mathbf{6}_0$	<i>3.026</i>	0.570	$\mathbf{6}_0^+$	<i>2.040</i>	0.655
$\mathbf{6}_1$	<i>3.054</i>	0.640	$\mathbf{6}_1^+$	<i>2.137</i>	0.728
$\mathbf{6}_2$	<i>3.085</i>	0.792	$\mathbf{6}_2^+$	<i>2.221</i>	0.831
$\mathbf{6}_3$	<i>3.114</i>	0.925	$\mathbf{6}_3^+$	<i>2.288</i>	0.933
$\mathbf{6}_4$	<i>3.140</i>	1.037	$\mathbf{6}_4^+$	<i>2.344</i>	1.030

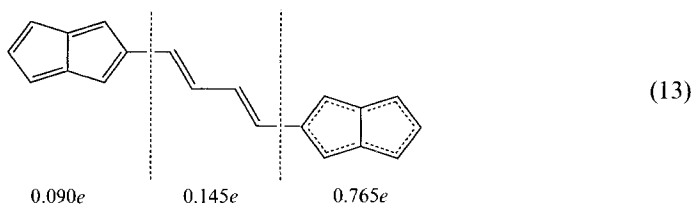
more, λ_{\max} values increase slightly as the polyethylene chain lengthens. Accordingly, all the molecules $\mathbf{6}_n$ and all radical cations $\mathbf{6}_n^+$ show pronounced second-order DBL. (The remaining eigenvalues λ_i , of which $\lambda_{\max-1}$ is given in Table 2, are all much smaller than $\lambda_{\text{critical}}$.)

The two eigenvectors $\mathbb{W}_{\max,1}$ and $\mathbb{W}_{\max,2}$, belonging to the degenerate eigenvalue λ_{\max} , are essentially the same for all $\mathbf{6}_n$ and $\mathbf{6}_n^+$. They may be chosen to have non-zero components in either of the two pentalene units and zero values in the other. For example, the eigenvector $\mathbb{W}_{\max,1}$ and $\mathbb{W}_{\max,2}$ of the radical cation $\mathbf{6}_1^+$ are:



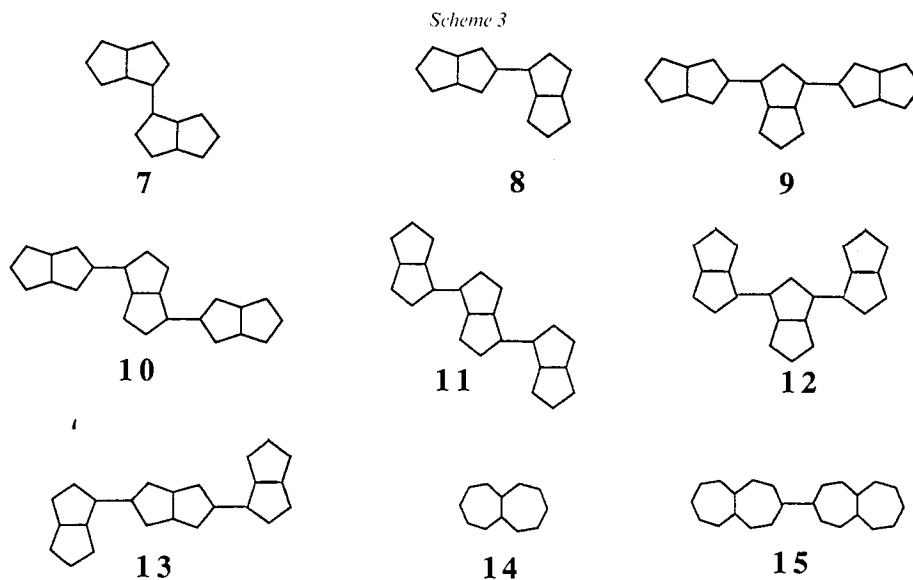
They are very similar to those of $\mathbf{3}$ (and thus of $\mathbf{3}^+$) shown in (6). As before, other solutions are obtained by forming linear combinations. Consequently, here too second-order DBL is delocalized and fluctuating. The polyethylene chain is not affected by second-order DBL, so that the bond orders $p_{\mu\nu}$ obtained from the standard *Hückel* calculation are still valid.

The charge-distribution analysis yields the following summed positive charges on the two pentalene and the central diene moieties for the radical cation $\mathbf{6}_2^+$ for the solution where second-order DBL is concentrated on one of the pentalene units.



Although the polyene moiety in the 6_n^+ systems seems to act mostly as a spacer (because the charge propagation will oscillate mainly between the pentalene units), its role as a conjugating link is important. For example, the λ_{\max} values of pentalene ($\lambda_{\max} = 2.357$) and 2-vinylpentalene ($\lambda_{\max} = 2.385$) are essentially the same, whereas that of 1,2-di(pentalen-2-yl)ethene ($\lambda_{\max} = 3.054$) is significantly larger. For the corresponding radical cations, one finds $\lambda_{\max} = 1.358$, $\lambda_{\max} = 1.500$, and $\lambda_{\max} = 2.137$, respectively. Thus, the polyene moieties are not inactive spacers, even if their bond lengths are not affected by second-order DBL.

6. Dependence of Fluctuating DBL on Connectivity. – We now show how the phenomenon of fluctuating DBL depends on the type of connectivity, using once more pentalene units as building blocks. *Scheme 3* shows the molecule types we have examined. In *Table 3* are collected the λ_i values larger than 1.6, assumed to be a lower limit for $\lambda_{\text{critical}}$. In addition, the HOMO/LUMO gap $\Delta x = (\epsilon_{\text{LUMO}} - \epsilon_{\text{HOMO}})/\beta$, and the symmetries of the HOMO, the LUMO, and the second-order DBL distortion mode are given for each molecule.



Earlier, we explained the presence of fluctuating DBL in 2,2'-bipentalenyl **3** in terms of a degenerate pair of LUMOs, separated by a small energy gap from the HOMO⁴). The degeneracy of the LUMOs of **3** is due to the fact that the connected centres C(2) and C(2') of the pentalene units lie on a nodal plane of the pentalene LUMO, as shown in (9). In contrast, when the pentalene units are joined at C(1) and C(1'), where the LUMO coefficients are non-zero, the resulting LUMOs of the dimer **7** are no longer degenerate, as illustrated in (14). Accordingly, λ_{\max} of **7** is not degenerate, and the second-order DBL does not fluctuate without activation energy. However, as the second largest λ_i is close to λ_{\max} , the activation energy will be rather small.

⁴) We caution that a small HOMO/LUMO gap is a necessary, but not a sufficient condition for second-order DBL. For example, fulvalene ($\Delta x = 0.311$) and heptafulvalene ($\Delta x = 0.174$) yield $\lambda_{\max} = 1.102$ and 1.216 respectively, and are thus stable with respect to second-order DBL. This reflects the occasional failure of the pseudo-Jahn-Teller argument [11] to predict the distortive behavior of molecules.

Table 3. Eigenvalues λ_i of the Bond-Bond Polarizability Matrices $\mathbf{\lambda}(n)$ of a Series of Closed-Shell Examples, Their DBL Patterns, Orbital Gaps, and Symmetry Behavior of the Relevant Inner Orbitals

No. ^{a)}	Symmetry ^{b)}	λ_i ^{c)}	DBL-Type ^{d)}	$-\Delta x$ ^{e)}	HOMO ^{f)}	LUMO ^{f)}	Dist. ^{g)}
1	D_{2h}	2.357	(1) L	0.471	B_{1u}	A_u	B_{1g}
3	D_{2h}	3.026	(2) DL; LD	0.206	B_{3g}	$B_{2g}; A_u$	$B_{1g}; B_{3u}$ fluct.
7	C_{2h}	2.619	(1) LL	0.256	B_g	A_u	B_u
8	C_s	1.767	(1) $D_I L_{II}^{h)}$	0.434	A''	A''	A'
		1.636	(1) $L_I D_{II}^{h)}$	0.531	A''	A''	A'
9	C_{2v}	1.947	(2) LDD; DDL	0.371	B_1	$A_2; B_1$	$B_2; A_1$ fluct.
10	C_{2h}	2.075	(2) LDD; DDL	0.332	B_g	$B_g; A_u$	$A_g; B_u$ fluct.
11	C_{2h}	2.773	(1) LLL	0.178	A_u	A_u	A_g
		2.626	(1) LLL	0.513	A_u	B_g	B_u
		2.153	(1) LLL	0.801	A_u	A_u	A_g
		2.750	(1) LLL	0.188	B_1	A_2	B_2
12	C_{2v}	2.465	(1) LLL	0.453	B_1	B_1	A_1
		2.411	(1) LLL	0.820	B_1	A_2	B_2
		1.787	(1) $LDL^j)$	0.429	A_u	$A_u; B_g$	A_g
13	C_{2h}	1.768	(1) $LDL^j)$				B_u
		2.595	(1) L	0.311	B_{3g}	B_{2g}	B_{1g}
15	D_{2h}	2.859	(2) LD; DL	0.174	B_{3g}	$B_{2g}; A_u$	$B_{1g}; B_{3u}$ fluct.

a) The numbers refer to the molecules depicted in *Scheme 3*.

b) Symmetry of the molecule under the assumption of coplanarity.

c) Only those λ_i values are given which satisfy the condition $\lambda_i > 1.6$, where the latter value is taken as a lower limit for $\lambda_{\text{critical}}$. The λ_{max} values are given in italics.

d) The values in parentheses is the degeneracy of the λ_i value. The second-order DBL pattern of each moiety is denoted by D (delocalized) or L (localized). The sequence of the symbols corresponds to the sequence of the pentalene subunits in the corresponding molecule.

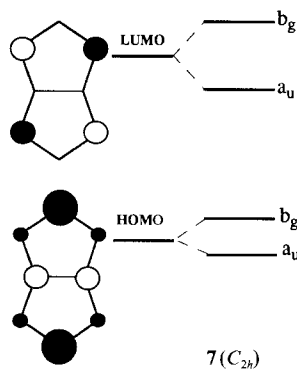
e) The top orbital gap is defined as $\Delta x = (\epsilon_{\text{LUMO}} - \epsilon_{\text{HOMO}})/\beta$ (italics), and the following ones as $\Delta x = (\epsilon_{\text{LUMO}+1} - \epsilon_{\text{HOMO}})/\beta$ and $\Delta x = (\epsilon_{\text{LUMO}+2} - \epsilon_{\text{HOMO}})/\beta$.

f) Irreducible representations of the HOMO, of the (accidentally degenerate) LUMOs, and of the LUMO+1, LUMO+2.

g) Symmetry of the DBL distortion pattern. It corresponds, with exception of **13**, to the product of the irreducible representations of the determining orbital pair (see text).

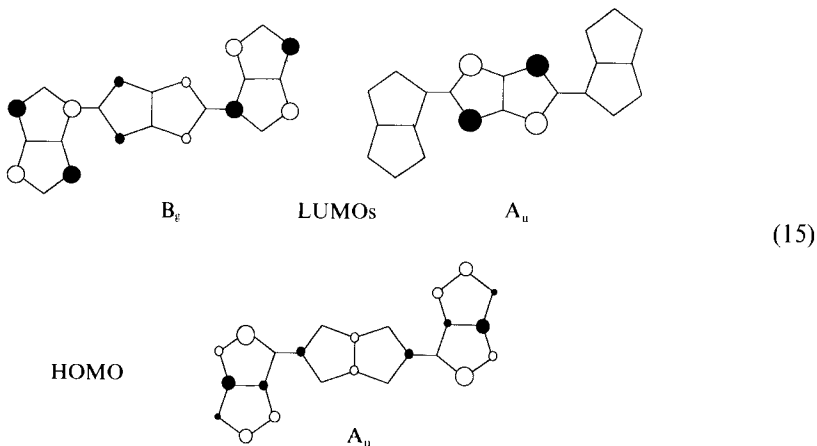
h) The lower indices of the symbols D and L refer to the pentalene moieties of **8**, as indicated in *Scheme 3*.

i) These λ_{max} and $\lambda_{\text{max}-1}$ values are slightly split, notwithstanding the accidental degeneracy of the ϵ_{LUMO} values. See text.

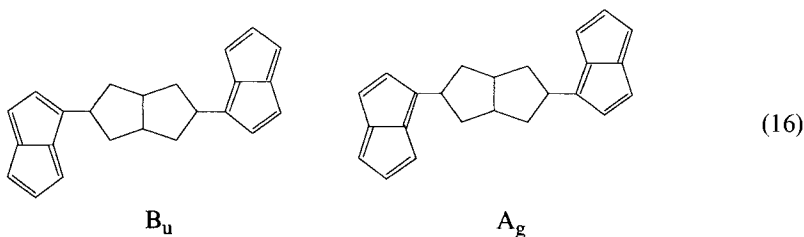


By the same argument, 1,2'-bipentalenyl **8** has a nondegenerate LUMO, and, accordingly, a non-degenerate λ_{\max} . In this case, the pentalen-2-yl moiety has a greater tendency to localize its double-bonds than the pentalen-1-yl unit, in accord with the size of the corresponding HOMO/LUMO and HOMO/LUMO+1 orbital-energy gaps.

The terpentalenyl systems **9** to **13** have been limited to those of at least C_{2v} or C_{2h} symmetry, in which the three pentalene units can assume a coplanar conformation (*i.e.* excluding the overcrowded 2,1':6',2''- and 1,1':6',1''-periterpentalenyls). They are the first members of polyterpentalenyl chains of type A-A-A-A... or A-B-A-B-A... Of these, only **9** and **10**, which have pentalen-2-yl 'end groups', have a degenerate λ_{\max} , and are thus truly fluctuating in the sense described for **3** to **6**, and their radical cations. The remaining ones, where the 'end groups' are pentalen-1-yl moieties, behave similarly to **8** and **9**. A particular interesting case is **13** which is non-fluctuating although its LUMOs (**15**) are acciden-



tally degenerate. However, these LUMOs are no longer related to each other by symmetry, as they are in (**9**) for **3**. Whereas the B_g LUMO has large coefficients on the outer pentalene units, the A_u LUMO is concentrated on the central one. On the other hand, the LUMO+1 of **13** is essentially the in-phase combination of the outer pentalene LUMOs, and thus A_u . According to our product rule, the distortion of type A_u ($\text{LUMO}+1 \otimes A_u(\text{HOMO}) = A_g$) is predicted to be somewhat less favorable than $B_g(\text{LUMO}) \otimes A_u(\text{HOMO}) = B_u$, in agreement with the result from the computation:



Thus, the rule of thumb, regarding the relationship between the degeneracies of the LUMOs and of the λ_{\max} values of a molecule, should be exercised with some care.

Table 3 also includes heptalene **14**, which has a strong tendency towards DBL of the bond-alternating type, and its dimer 3,3'-biheptalenyl **15**, which also exhibits fluctuating DBL, in analogy to **3**. The analogy also holds with respect to the degeneracy of the pair of LUMOs of **15**, which is caused by the connected C(3) and C(3') lying on a node of the heptalene LUMO.

To summarize, it is possible to rationalize – within obvious limits – the above observations in terms of the simple rules of thumb given in *Chapt. 2* and *3*, namely,

A) that the smaller the orbital gap $\Delta x = (\varepsilon_{\text{LUMO}} - \varepsilon_{\text{HOMO}})/\beta$ between the HOMO and the LUMO(s), the stronger the tendency towards second-order DBL, *i.e.* the larger λ_{max} ,

B) that a pair of degenerate LUMOs (or, as the case may be, of HOMOs) will usually lead to degenerate λ_{max} values, and thus to fluctuating DBL, and

C) that the product of the irreducible representations of the inner orbitals will correspond, more often than not, to the type of second-order DBL distortion. However, as is usual for such rules of thumb, they have their exceptions, as we have seen in the case of **13**.

Notwithstanding their limitations, our rules of thumb suggest at least, which types of building blocks are liable to yield oligomers with fluctuating DBL.

7. Concluding Remarks. – At the level of a HMO perturbation theory, some systems have a low-energy pathway for charge-density migration. Such systems include radical cations built from pentalene units, linked at C(2) and C(2') either directly or *via* a polyene chain. In contrast to pentalene itself – where DBL takes the form of bond alternation, and where the switch from one localization pattern to the other proceeds through a symmetric, delocalized, high-energy transition state – the fluctuating DBL and charge migration in these molecules proceeds without activation energy, and avoids the more symmetric delocalized structure. Polyheptalenyls behave in the same manner, if the heptalene units are linked through their 3- and/or 8-positions. This is reminiscent of the charge migration in the benzene radical cation undergoing *Jahn-Teller* distortions, as first discussed by *Moffitt* and *Liehr* [15].

The charge propagation in the corresponding radical cations exhibits two interesting features. In the polypentalenyls consisting of N pentalene units, the excess positive charge has a tendency to settle on the central ring, if N is odd, or to migrate mainly between the two central rings, if N is even, and it needs a small activation energy to move towards the terminal pentalene moieties. On the other hand, when two pentalenes are separated by a polyene chain, the charge transfer, accompanying the passage from one extreme DBL structure to the other, is more like a classical electron-transfer process [16], involving intermediate DBL structures.

Simple rules involving the symmetry behavior of the LUMOs and HOMOs of these molecules⁵⁾ and the size of the gap between their orbital energies appear to allow a rationalization of most of the results. They should prove to be useful for designing molecules exhibiting activation-energy-free fluctuating DBL. Similar mechanisms involv-

⁵⁾ It is noteworthy that the graphs \mathfrak{G} of those molecules and radical cations mentioned above, which exhibit fluctuating DBL, belong from a topological point of view to the group D_4 [17]. As a consequence, their line-graph $\mathfrak{L}(\mathfrak{G})$, representing the underlying symmetry of the bond-bond polarizability matrix \mathfrak{P} , belongs to the same group, which allows degenerate eigenvalues λ_i . It is not *a priori* evident that λ_{max} should be one of them.

ing electron transfer without activation energy may operate in other classes of compounds, relevant in material science, memory switches, or superconductivity.

Our thanks go to Prof. *J. D. Dunitz* (ETH-Zürich) and to Prof. *L. Salem* (Université de Paris) for their helpful suggestions and constructive criticisms. Needless to say that they are in no way responsible for the shortcomings of this contribution.

Appendix. – For a given π system, extending over n $2p$ centres and having a topography characterized by a simple graph \mathfrak{G} , belonging to the (maximal) symmetry point-group G , one first computes the HMOs

$$\varphi_j = \sum_{\mu} \phi_{\mu} c_{\mu j} \quad (\text{A1})$$

and the corresponding orbital energies

$$\varepsilon_j = \alpha_0 + \beta_0 x_j \quad (\text{A2})$$

according to standard HMO practice, setting all $\alpha_{\mu} = \alpha_0$ and all $\beta_{\mu\nu} = \beta_0$ for bonded centres μ, ν . The x_j are the eigenvalues of the adjacency matrix \mathfrak{A} of the graph \mathfrak{G} . The total π energy is

$$E_{\pi,0} = \sum_j b_j \varepsilon_j = N_e \alpha_0 + \beta_0 X_{\pi,0}, \quad (\text{A3})$$

where the b_j are the occupation numbers of the orbitals φ_j in the given electronic configuration Φ of the molecule. $N_e = \sum_j b_j$ is the number of π electrons, and $X_{\pi,0} = \sum_j b_j x_j$.

First-order DBL is determined by the bond orders

$$p_{\mu\nu} = \sum_j b_j c_{\mu j} c_{\nu j}. \quad (\text{A4})$$

In a crude approximation, the first-order equilibrium bond lengths $R_{\mu\nu}^0$ are then given by

$$R_{\mu\nu}^0 = R_0 + r(p_{\mu\nu} - 2/3), \quad (\text{A5})$$

where R_0 is the length of a π bond in benzene, and $2/3$ the value of the corresponding bond order. The parameters R_0 and r are empirically calibrated by comparison with observed bond lengths:

$$R_{\mu\nu}^0/p_{\mu\nu} \approx 140 - 17(p_{\mu\nu} - 2/3). \quad (\text{A6})$$

Note that first-order DBL always conserves the full (maximal) symmetry G of the graph \mathfrak{G} , and thus of the π system.

We now move the reference point for our calculation from $R_{\mu\nu} = R_0$ to $R_{\mu\nu} = R_{\mu\nu}^0$ for each bond μ, ν . The total energy at this point is then $E_{\text{tot}}^0 = E_{\sigma}^0 + E_{\pi}^0$. For small changes in bond-lengths, $\delta R_{\mu\nu} = R_{\mu\nu} - R_{\mu\nu}^0$, the total energy E_{tot} can be developed around E_{tot}^0 , according to

$$E_{\text{tot}} = E_{\text{tot}}^0 + (1/2) \sum_{\mu\nu} k \delta R_{\mu\nu}^2 + (1/2) \sum_{\mu\nu} \sum_{\rho\sigma} (\partial^2 E_{\pi} / \partial R_{\mu\nu} \partial R_{\rho\sigma}) \delta R_{\mu\nu} \delta R_{\rho\sigma} + \text{higher terms}. \quad (\text{A7})$$

Assuming that in the interval of interest, $\beta_{\mu\nu}$ is a linear function of the interatomic distance $R_{\mu\nu}$, i.e. $\partial^2 \beta_{\mu\nu} / \partial^2 R_{\mu\nu} = 0$, then the part of (A7) in parentheses becomes [7]

$$(\partial^2 E_{\pi} / \partial R_{\mu\nu} \partial R_{\rho\sigma}) = 2\beta^{-1} \pi_{\mu\nu,\rho\sigma} (\partial \beta_{\mu\nu} / \partial R_{\mu\nu}) (\partial \beta_{\rho\sigma} / \partial R_{\rho\sigma}), \quad (\text{A8})$$

where the $\pi_{\mu\nu,\rho\sigma}$ are the bond-bond polarizabilities of the π system computed according to

$$\pi_{\mu\nu,\rho\sigma} = \beta \sum_j \sum_{k \neq j} b_j \frac{(c_{\mu j} c_{\nu k} + c_{\mu k} c_{\nu j})(c_{\rho j} c_{\sigma k} + c_{\rho k} c_{\sigma j})}{\varepsilon_j - \varepsilon_k} \quad (\text{A9})$$

As defined in (A9), the $\pi_{\mu\nu,\rho\sigma}$ are pure numbers, i.e. $\dim(\pi_{\mu\nu,\rho\sigma}) = 1$.

The dependence of $\beta_{\mu\nu}$ on the interatomic distance $R_{\mu\nu}$ can be roughly estimated from PE spectroscopic data of aromatic hydrocarbons [18], polyenes [19], and polyynes [20]. Assuming that this dependence is linear within the range of interatomic distances covered in our treatment, one obtains $\partial \beta_{\mu\nu} / \partial R_{\mu\nu} \approx 0.13 \text{ eV pm}^{-1}$. In conjunction with (A6), this leads to

$$\partial \beta_{\mu\nu} / \partial p_{\mu\nu} \approx -2.2 \text{ eV}. \quad (\text{A10})$$

To assess whether the molecule undergoes second-order DBL towards one or the other of its *Kekulé* structures, or towards some other pattern with pronounced bond alternation, we first compute the bond-bond polarizabilities $\pi_{\mu\nu,\rho\sigma}$ of the N bonds of the π system according to (A9), and collect them in a symmetric $N \times N$

matrix $\boldsymbol{\pi} = (\pi_{\mu\nu,\rho\sigma})$, with the index pairs μ, ν in the sequence $1, 1; 1, 2; \dots; 1, \mu \dots 1, N; 2, 1; 2, 2; \dots; 2, \mu \dots 2, N$; etc. Solving the eigenvalue/eigenvector problem

$$\boldsymbol{\pi} \boldsymbol{w} = \lambda \boldsymbol{w} \quad (\text{A11})$$

yields N positive eigenvalues

$$\lambda_1 < \lambda_2 < \dots < \lambda_i < \dots < \lambda_N = \lambda_{\max} \quad (\text{A12})$$

and the corresponding column eigenvectors

$$\boldsymbol{w}_i = (u_{i,\mu\nu})^T \quad (\text{A13})$$

It can be shown [7] that second-order DBL occurs within our model, if

$$\lambda_{\max} > \lambda_{\text{critical}} = k |\beta_0| / |\beta'_0|^2 \quad (\text{A14})$$

where k is the (mean) σ -bond force constant assuming a harmonic potential $V_\sigma(R_{\mu\nu})$, β_0 the resonance integral, and β'_0 its derivative $(d\beta/dR)_0$ (both for the interatomic distance R_0). If (A14) is satisfied, second-order DBL proceeds according to the irreducible representation $\Gamma(\boldsymbol{w}_{\max})$ of G , to which the eigenvector $\boldsymbol{w}_{\max} = (u_{\max,\mu\nu})^T$ of λ_{\max} belongs. In addition, the individual components yield a first approximation of the relative sign and size of the expected changes in bond-length $R_{\mu\nu}$.

As far as the criterion (A14) is concerned, it can be shown that $\lambda_{\text{critical}} = 1.7$ to 1.8 is a reasonable value [7]. Thus, a molecule with $\lambda_{\max} > 1.7$ to 1.8 will undergo second-order DBL, whereas molecules with $\lambda_{\max} < 1.7$ to 1.8 will conserve their first-order, fully symmetric delocalized structure.

Although the procedure tells us, whether a molecule will undergo spontaneous DBL, and which of the bonds are going to contract or lengthen, it cannot provide values for the final equilibrium bond-lengths $R_{\mu\nu,\text{eq}}$, because these depend on higher-order terms not included in the treatment, and on the unharmonicity of the true σ potential $V_\sigma(R_{\mu\nu})$. However, a reasonable approximation for the equilibrium bond-orders is provided by the formula

$$p_{\mu\nu,\text{eq}} = p_{\mu\nu} + f_{\text{eq}} \cdot u_{\max,\mu\nu} \quad (\text{A15})$$

where f_{eq} is a factor, roughly in the range of $1 > f_{\text{eq}} > 1/2$. Using (A6), (A10), and (A15) one finds

$$\beta_{\mu\nu,\text{eq}} = \beta_0(1 + 0.66(p_{\mu\nu} - 2/3) + 0.66 \cdot f_{\text{eq}} \cdot u_{\max,\mu\nu}). \quad (\text{A16})$$

Setting $\beta_{\mu\nu,\text{eq}}/\beta_0 = 1 + \delta_{\mu\nu,\text{eq}}$ for practical reasons, one obtains in a sufficient approximation, which we shall use in this work:

$$\delta_{\mu\nu,\text{eq}} \approx (2/3)(p_{\mu\nu} - 2/3) + u_{\max,\mu\nu}/2 \quad (\text{A17})$$

Using these values within a further HMO calculation, one obtains the orbitals (A1) of the molecule, including first and second-order DBL. These allow a discussion of the charge redistribution within the molecule, which accompanies DBL.

As this discussion is to be carried out on a HMO level, it is useful to remind oneself of some of the peculiar features of the HMO model. From the coefficients $c_{\mu j}$ of the linear combinations (A1), one calculates the bond-orders (A4) and the charge orders

$$q_\mu = \sum_j b_j c_{\mu j}^2 \quad (\text{A18})$$

which define the π -electron charge

$$Q_\mu = -e q_\mu \quad (\text{A19})$$

at the centre μ , i.e. the charge within the space spanned by the basis orbital ϕ_μ . Only if this space is the same for all ϕ_μ , then the π -electron densities at the different centres μ are proportional to q_μ .

The bond-orders $p_{\mu\nu}$ are not associated with local charges $Q_{\mu\nu}$ between the centres, because these are defined as

$$Q_{\mu\nu} = -e 2p_{\mu\nu} S_{\mu\nu} \quad (\text{A20})$$

i.e. in a model with non-orthogonal basis functions. However, in our HMO model the ϕ_μ are assumed to form an orthogonal set, so that $Q_{\mu\nu} = 0$, because $S_{\mu\nu} = 0$. (It follows that in a HMO model $\sum_\mu q_\mu = N_e =$ number of π electrons.) As a consequence, in a HMO model, charge transfer involves only changes in Q_μ .

Our treatment for second-order DBL takes care of the above features. It neglects the changes in Q_μ . This is the reason why we are using only the bond-bond polarizability matrix $\boldsymbol{\pi} = (\pi_{\mu\nu,\rho\sigma})$, and do not include the atom-atom and atom-bond polarizabilities.

REFERENCES

- [1] H. Labhart, *J. Chem. Phys.* **1957**, *27*, 157; Y. Ooshika, *J. Phys. Soc. Jpn.* **1957**, *12*, 1238, 1248; H.C. Longuet-Higgins, L. Salem, *Proc. R. Soc. London [Ser.] A* **1959**, *251*, 172; *ibid.* **1960**, *257*, 445; P.C. den Boer-Veenendaal, D.H.W. den Boer, *Mol. Phys.* **1961**, *4*, 33; T. Nakajima, S. Katagiri, *ibid.* **1963**, *7*, 149; W. Kutzelnigg, *Theor. Chim. Acta* **1966**, *4*, 417; W. Kutzelnigg, 'Einführung in die Theoretische Chemie', Verlag Chemie, Weinheim-New York, 1978, Vol. II, p. 308–318.
- [2] K. Hafner, H.U. Süss, *Angew. Chem.* **1973**, *85*, 626; *ibid. Int. Ed.* **1973**, *12*, 575.
- [3] B. Kitschke, H.J. Lindner, *Tetrahedron Lett.* **1977**, 2511.
- [4] L. Ebersson, 'Electron Transfer Reactions in Organic Chemistry', Springer Verlag, Heidelberg, 1987.
- [5] R.D. Canon, 'Electron Transfer Reactions', Butterworths, London, 1980.
- [6] J.Y. Becker, J. Bernstein, S. Bittner, Eds., 'The Chemistry of Organic Conductors', *Isr. J. Chem.* **1986**, *27*.
- [7] G. Binsch, E. Heilbronner, J.N. Murrell, *Mol. Phys.* **1966**, *11*, 305; G. Binsch, E. Heilbronner, in 'Structural Chemistry and Molecular Biology: A Volume Dedicated to Linus Pauling by his Students, Colleagues and Friends', Eds. A. Rich and N. Davidson, Freeman and Co., San Francisco, 1968; G. Binsch, E. Heilbronner, *Tetrahedron* **1968**, *24*, 1215.
- [8] G. Binsch, I. Tamir, R.D. Hill, *J. Am. Chem. Soc.* **1969**, *91*, 2446; G. Binsch, I. Tamir, *ibid.* **1969**, *91*, 2450.
- [9] A.L. Chung, M.J.S. Dewar, *J. Chem. Phys.* **1965**, *42*, 756; M.J.S. Dewar, G.J. Gleicher, *J. Am. Chem. Soc.* **1965**, *87*, 685, 692, 4414; *Tetrahedron* **1965**, *21*, 1817, 3423; *Tetrahedron Lett.* **1965**, *50*, 4503.
- [10] E. Heilbronner, Z.-Z. Yang, *Angew. Chem.* **1987**, *99*, 369; *ibid. Int. Ed.* **1987**, *26*, 360.
- [11] D.H.W. den Boer, P.C. den Boer, H.C. Longuet-Higgins, *Mol. Phys.* **1962**, *5*, 387; L. Salem, 'Electrons in Chemical Reactions', Wiley-Interscience, New York, 1982, p.174; T.A. Albright, J.K. Burdett, M.H. Whangbo, 'Orbital Interactions in Chemistry', Wiley-Interscience, New York, 1985, p.95–97.
- [12] T. Nakajima, A. Toyota, S. Fujii, *Bull. Chem. Soc. Jpn.* **1972**, *45*, 1022.
- [13] L. Salem, J. Durup, C. Bergeron, D. Cazes, X. Chapuisat, L. Kagan, *J. Am. Chem. Soc.* **1970**, *92*, 4472; L. Salem, *Acc. Chem. Res.* **1971**, *4*, 322.
- [14] V. Bonacic-Koutecky, P. Bruckmann, P. Hiberty, J. Koutecky, C. Leforestier, L. Salem, *Angew. Chem.* **1975**, *87*, 599; *ibid. Int. Ed.* **1975**, *14*, 575.
- [15] W. Moffitt, A.D. Liehr, *Phys. Rev.* **1957**, *106*, 1195; A.D. Liehr, *Rev. Mod. Phys.* **1960**, *32*, 346; see also: L. Salem, 'The Molecular Orbital Theory of Conjugated Systems', W. A. Benjamin, New York, 1966.
- [16] R.A. Marcus, *Ann. Rev. Phys. Chem.* **1964**, *15*, 155.
- [17] J.D. Dunitz, 'X-Ray Analysis and the Structure of Organic Molecules', Cornell University Press, Ithaca, 1979, p.463.
- [18] R. Boschi, E. Clar, W. Schmidt, *J. Am. Chem. Soc.* **1974**, *60*, 4406; W. Schmidt, *ibid.* **1977**, *66*, 828, and ref. cit. therein.
- [19] M. Beez, G. Bieri, H. Bock, E. Heilbronner, *Helv. Chim. Acta* **1973**, *56*, 1028; E. Heilbronner, J.P. Maier, 'Some Aspects of Organic Photoelectron Spectroscopy', in 'Electron Spectroscopy; Theory, Techniques and Applications', Eds. C.R. Brundle and A.D. Baker, Academic Press, London, 1977, and ref. cit. therein.
- [20] E. Heilbronner, V. Hornung, J.P. Maier, E. Kloster-Jensen, *J. Am. Chem. Soc.* **1974**, *96*, 4252; M. Allen, E. Heilbronner, E. Kloster-Jensen, J.P. Maier, *Chem. Phys. Lett.* **1976**, *41*, 228; G. Bieri, E. Heilbronner, T.B. Jones, E. Kloster-Jensen, J.P. Maier, *Phys. Scr.* **1977**, *16*, 202.